

Probabilistic Predictions of Penetrating Injury to Anatomic Structures*

Omolola Ogunyemi, M.S.E., Bonnie Webber, Ph.D.,
Center for Human Modeling and Simulation,
Univ. of Pennsylvania, Philadelphia, PA 19104-6389
John R. Clarke, M.D., FACS

Dept. of Surgery, Allegheny University of the Health Sciences, Philadelphia, PA 19129

This paper presents an interactive 3D graphical system which allows the user to visualize different bullet path hypotheses and stab wound paths and computes the probability that an anatomical structure associated with a given penetration path is injured. Probabilities can help to identify those anatomical structures which have potentially critical damage from penetrating trauma and differentiate these from structures that are not seriously injured.

INTRODUCTION

Assessing the type and magnitude of injuries involved in penetrating trauma from gunshot and stab wounds requires a working knowledge of the relationship between human anatomy, physiology, and physical manifestations of injury. With ballistic injuries involving multiple entry and exit wounds, these assessments are even more difficult because the same external wounds could be produced by many different bullet paths. In [11], we described a 3D graphical penetration path assessment system which enables users to visualize different bullet path hypotheses as well as stab wound paths and to identify the anatomical structures affected for each path, using a rotatable 3D model of a human torso. This system has now been extended to present the degree of belief that an anatomical structure associated with a given penetration path is injured, expressed as a probability (within confidence limits). In addition, a more realistic, continuous curve, wound path representation for ballistic injuries has been created, and a simple model of bullet ricochet off skeletal structures has been developed.

By displaying injured organ possibilities and associated penetration probabilities for a given set of wounds, the system provides a visual cue to their potential consequences, and in this way could aid medical professionals in reducing the injury hypotheses under consideration. System functionality includes through-body navigations which enable the user to follow a penetration path in virtual space through the structures it affects.

*This work has been supported by the NLM under contract number NOI-LM-4-3515, and ARPA under grant number DAMD17-94-J-4486. The authors would like to thank Jonathan Kaye, Rich Washington, Dr. Abba Krieger and Harold Sun for their assistance.

In this way, the system serves a function similar to that of a CT-scan, with the added benefit of quantitative information in the form of probabilities that describe the likelihood of damage to anatomical structures.

The penetration path assessment system presents an initial space of penetration possibilities*; ballistic characteristics such as bullet type and velocity are not considered in assessing injuries from gunshot wounds. Although the system can model bullet ricochet off skeletal parts, it does not address such issues as bullet fragmentation and the impact of secondary projectiles from bullet or bone fragments. For an examination of these and other related issues, see [3, 4, 5, 6, 13, 14, 15].

The organ, skeleton, and skin models currently used are polygonal surface models developed at Viewpoint DataLabs. Polygonal surface models of major blood vessels were developed in-house based on reconstructions from CT-scan data using SPAMMVU and descriptions from anatomy texts [1, 7, 8]. The current torso model is a fixed-size model of an "average" female. Our methods for calculating penetration probabilities are independent of the particular anatomical models used.

WOUND REPRESENTATIONS

Definitions

Possible injury to anatomical structures is determined using 3D models of both penetration paths and anatomical structures. We refer to the 3D models of penetration paths as *wound path spaces*. For gunshot wounds, a wound path space is the space of possible trajectories from an entry wound to an exit wound, a bullet lodged in the body, or a skeletal nick. For stab wounds, it is the area potentially affected by the instrument used in a stabbing.

A *penetration path hypothesis* consists of one or more gunshot wound path spaces, depending on the number of gunshot wounds.

*Diagnosis follows from both penetration possibilities and the signs and symptoms observed in a patient. For example, suspicion of lung penetration accompanied by distended neck veins and decreased breath sounds might lead to a diagnosis of tension pneumothorax.



Figure 1: Gunshot wound path space

Gunshot wound representation

Previously, we described the wound path space representation for gunshot wounds as two cones joined at their bases [11]. This gave rise to bullet trajectory models with sharp discontinuities corresponding to the meeting point of the cones' bases. We have since replaced this model with a more realistic, continuous curve representation (see Figure 1). Each wound path space is oriented in such a way that one apex corresponds to an entry wound location and the other to an exit wound, bullet, or skeletal nick (in the case of ricochet). The wound path space model combines hypotheses about the possible paths taken by a bullet with information about potential cavitation effects that result from its movement through body tissue. The ratio of the model's length to its diameter is fixed at 100:18, based on values obtained from [2, 3] of the dimensions of permanent and temporary wound cavities produced in injuries involving projectiles. The wound path space representation reflects the maximum expected deviation (from a straight line path) of any continuous line trajectory.

To model the region affected in the case of bullet ricochet off bone, we consider two pairings – one from an entry wound to a particular area of the skeleton and another from this area of the skeleton to either a bullet lodged in the body or an exit wound. The result is two wound path spaces like the one in Figure 1 joined end to end: one wound path space has an apex at the location of the entry wound and its other apex at the area of the skeleton nicked by the bullet. The second wound path space has one apex at the skeletal nick and its other apex at either a bullet location or an exit wound location.

Stab wound representation

Two simplifications are made in modeling the wound path space for a stab wound:

1. We assume it comes from a fixed length blade,
2. We constrain the possible directions of penetration of the blade by placing the wound path space perpendicular to the skin surface at the point of the stabbing[†].

[†] This constraint could be relaxed with more information from the user in future versions of the system



Figure 2: Stab wound path space

The wound path space representation for a stab wound is a truncated cone or frustum (Figure 2), with its smaller base positioned at the blade's entry point, and its wider base placed internally in such a way that the frustum is perpendicular to the skin surface. The "vee" shape of the wound path space reflects uncertainty about the limits of the direction of penetration of the blade to the left and right of the axis perpendicular to the blade's entry point on the skin surface, and the wound path space's circularity represents uncertainty about the orientation of the blade about the axis perpendicular to the entry point on the skin surface.

CALCULATING INJURY PROBABILITIES

Our previous article explains in detail how we determine which anatomical structures might be injured for a given wound path space. Once this information is obtained, it is useful to know how likely it is that a structure associated with a particular wound path space was hit. We use probabilities to express the likelihood of involvement of anatomical structures in a penetrating injury. Since the penetration probabilities calculated are approximations, our calculations include upper and lower limits of confidence about the accuracy of each probability derived. The interval estimated by these confidence bounds is a range of probabilities that has a 95% chance of including the true penetration probability (it is a 95% confidence interval).

The hit probability for a given anatomical structure is calculated by generating a number of experimental trajectories or stab paths (within a wound path space that has already been determined to intersect the structure), and then computing how many of these trajectories or stab paths hit the structure in question. For each wound path space that intersects anatomical structures, an intersection check is performed between trajectories generated within the wound path space and all anatomical structures that intersect the wound path space. Each trajectory generated either intersects a structure (a hit) or does not (a miss). The total number of trajectories or stab paths that intersect an anatomical structure is represented by the binomial random variable X with parameters n and p , where n is the total number of experimental trajectories or stab paths generated and p the probability of a hit. The sample hit probability

for the anatomical structure, \bar{X} , is the total number of hits divided by the number of randomly generated trajectories:

$$\bar{X} = \frac{X}{n} \quad (1)$$

We use the sample hit probability, \bar{X} , as an estimate of p because it is an unbiased estimator for p (the true hit probability) [9].

We determine the confidence bounds for a given hit probability using a normal approximation to the binomial distribution. The confidence bounds for \bar{X} are given by:

$$\left(\bar{X} - z_{\alpha/2} \sqrt{\frac{\bar{X}(1 - \bar{X})}{n}}, \bar{X} + z_{\alpha/2} \sqrt{\frac{\bar{X}(1 - \bar{X})}{n}} \right) \quad (2)$$

where n is the number of simulated trajectories/stab-paths and $z_{\alpha/2}$ is the area under the standard normal density function from $-\infty$ to $z_{\alpha/2}$. The interval described by equation 2 corresponds to a $100(1 - \alpha)\%$ confidence interval. For on-screen display purposes, we write equation 2 as

$$\bar{X} \pm z_{\alpha/2} \sqrt{\frac{\bar{X}(1 - \bar{X})}{n}}$$

In order to produce a 95% confidence interval, α is set to 0.05 and the corresponding value for $z_{\alpha/2} = z_{0.025}$ is 1.960 [9, 10].

The process of generating experimental trajectories for gunshot wounds differs slightly from that for stab wounds since the mechanisms of injury lead to different wound path space models (Figures 1 and 2).

Generating experimental bullet trajectories

Our method for calculating hit probabilities for ballistic injuries involves simulating possible trajectories. To determine the number of trajectories to use for the probability calculations we estimated injury probabilities for the same set of external wounds and anatomical structures using different numbers, n , of trajectories, starting with $n = 50$. The difference in the endpoints of the confidence interval decreased at a rate inversely proportional to \sqrt{n} . Currently, we generate 200 trajectories for the purpose of calculating injury probabilities, but the number of trajectories simulated can easily be increased (at the expense of an increase in computation time).

Each trajectory extends from one apex of the wound path space to the other and is created from two randomly generated angles. One angle corresponds to the amount of a trajectory's deviation from a straight line

path and the other to its rotation about a given wound path space apex. The angle corresponding to the trajectory's deviation from a straight line path is produced using a random number generator (from the Free Software Foundation) that generates random numbers according to a normal distribution. The inputs to the random number generator are the mean angle and variance for the distribution, and in this case the mean is an angle of 0 degrees, corresponding to a straight line path (i.e., the average trajectory is one that does not deviate from a straight line path) and the variance corresponds to $(0.5 * MaxAngle)^2$, where $MaxAngle$ is the angle that represents the maximum deviation a trajectory can have from a straight line path while staying within the boundaries of the wound path space model.

The value for the variance is selected in keeping with two conventions:

- In a normal distribution, 95% of values in the distribution are expected to occur within two standard deviations of the mean of the distribution.
- In trauma care, injuries that have less than a 5% probability of being present (based on clinical information) are not pursued with costly definitive diagnostic procedures.

Since the standard deviation ($0.5 * MaxAngle$) is half of the two standard deviations from the center that would encompass 95% of bullet paths, we set the variance to be $(0.5 * MaxAngle)^2$. This choice of variance produces trajectories which stay within the boundaries of the wound path space model roughly 95% of the time and trajectories whose paths lie outside these boundaries roughly 5% of the time (see [12]).

The angle r representing a trajectory's rotation about a wound path space apex lies in the interval $0^\circ \leq r < 360^\circ$ and is produced using a random number generator which generates uniformly distributed numbers, x , over the interval $0.0 \leq x < 1.0$.

Generating experimental stab paths

To determine stab wound probabilities, we simulate a set of blades within the stab wound path space using two angles to determine the slant and rotation of the blade. One angle corresponds to the deviation of the blade from a direction perpendicular to the entry point on the skin surface and the other to the rotation of the blade about an axis perpendicular to the blade's entry point. The angles are generated in much the same way as those for the gunshot trajectories: the first is produced by the random number generator that obeys a normal distribution, and the second by the generator that obeys a uniform distribution. Currently we use 200

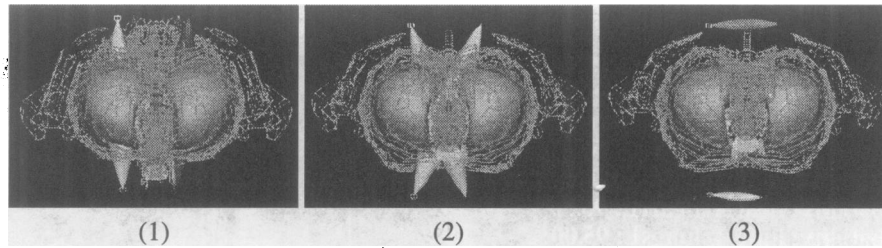


Figure 3: Cross-sectional views of three penetration path hypotheses

simulated blades for our anatomical structure intersection calculations. The number of blades used in intersection calculations may be increased but the attendant trade-off between accuracy in estimating probabilities and increases in computation time must be taken into consideration.

EXAMPLE

Consider a case involving four external gunshot wounds (two anterior, two posterior) to the left and right sides of the chest, and no bullets lodged in the body. There are three different penetration path hypotheses for these gunshot wounds (Figure 3). The text output below is the system's assessments of these hypotheses. Figure 4 shows output for hypothesis (1). The actual system display is in color - Figures 3 and 4 are black and white screen dumps.

```
(HYPOTHESIS 1)
Computing intersections for bullet/stab path #1
Skeleton parts in path: skeleton.lcartilage4
Skeleton parts in path: skeleton.lcartilage5
Skeleton parts in path: skeleton.sternumbody
Skeleton parts in path: skeleton.rib8
Skeleton parts in path: skeleton.t8
Organs in path: heartL.heartL
Organs in path: lungsL.lungsL
Organs in path: desc_aorta.desc_aorta
Organs in path: wind.pipes
Organs in path: wind.trachea

Hit probability: skeleton.lcartilage4: 96.00% +/- 2.72
Hit probability: skeleton.lcartilage5: 0.50%
Hit probability: skeleton.sternumbody: 4.50% +/- 2.87
Hit probability: skeleton.rib8: 95.00% +/- 3.02
Hit probability: skeleton.t8: 19.00% +/- 5.44
Hit probability: heartL.heartL: 93.50% +/- 3.42
Hit probability: lungsL.lungsL: 95.00% +/- 3.02
Hit probability: desc_aorta.desc_aorta: 20.50% +/- 5.60
Hit probability: wind.pipes: 23.00% +/- 5.83
Hit probability: wind.trachea: 25.50% +/- 6.04

Computing intersections for bullet/stab path #2
Skeleton parts in path: skeleton.rrib8
Organs in path: lungsL.lungsL
Organs in path: wind.pipes
Organs in path: wind.trachea

Hit probability: skeleton.rrib8: 96.00% +/- 2.72
Hit probability: lungsL.lungsL: 96.00% +/- 2.72
Hit probability: wind.pipes: 2.00%
Hit probability: wind.trachea: 2.00%

(HYPOTHESIS 2)
Computing intersections for bullet/stab path #1
Skeleton parts in path: skeleton.rrib8
Skeleton parts in path: skeleton.t7
Skeleton parts in path: skeleton.t8
Skeleton parts in path: skeleton.t9
Organs in path: wind.pipes
Organs in path: wind.esophagus
Organs in path: wind.trachea
Organs in path: heartL.heartL
Organs in path: lungsL.lungsL

Hit probability: skeleton.rrib8: 93.50% +/- 3.42
Hit probability: skeleton.t7: 3.00% +/- 2.36
```

```
Hit probability: skeleton.t8: 38.00% +/- 6.73
Hit probability: skeleton.t9: 4.00% +/- 2.72
Hit probability: wind.pipes: 21.50% +/- 5.69
Hit probability: wind.esophagus: 13.50% +/- 4.74
Hit probability: wind.trachea: 5.50% +/- 3.16
Hit probability: heartL.heartL: 98.50%
Hit probability: lungsL.lungsL: 96.00% +/- 2.72

Computing intersections for bullet/stab path #2
Skeleton parts in path: skeleton.rib8
Skeleton parts in path: skeleton.t7
Skeleton parts in path: skeleton.t8
Skeleton parts in path: skeleton.t9
Organs in path: desc_aorta.desc_aorta
Organs in path: wind.pipes
Organs in path: wind.esophagus
Organs in path: wind.trachea
Organs in path: heartL.heartL
Organs in path: lungsL.lungsL

Hit probability: skeleton.rib8: 94.00% +/- 3.29
Hit probability: skeleton.t7: 12.50% +/- 4.58
Hit probability: skeleton.t8: 96.00% +/- 2.72
Hit probability: skeleton.t9: 3.00% +/- 2.36
Hit probability: desc_aorta.desc_aorta: 2.50%
Hit probability: wind.pipes: 95.50% +/- 2.87
Hit probability: wind.esophagus: 93.00% +/- 3.54
Hit probability: wind.trachea: 9.50% +/- 4.06
Hit probability: heartL.heartL: 97.50%
Hit probability: lungsL.lungsL: 92.50% +/- 3.65

(HYPOTHESIS 3)
Computing intersections for bullet/stab path #1
No organ/skeleton intersections detected

Computing intersections for bullet/stab path #2
No organ/skeleton intersections detected
```

FUTURE WORK AND CONCLUSION

We have presented an interactive graphical system that determines which anatomical structures are affected in penetrating trauma and computes the probability of injury to these structures. The system can be used as a stand-alone system (to aid in diagnosis or help medical students in learning about anatomy), or it may be coupled to a rule-based or decision theoretic diagnostic reasoning system.

Coupling the assessment system to a diagnostic reasoner would give the latter principled evidence deriving from the mechanism of injury. Making the coupling bi-directional would allow feedback from the diagnostic reasoner to help the assessment system eliminate certain penetration path hypotheses. The assessment system could then increase penetration probabilities for anatomical structures associated with hypotheses that were not ruled out and decrease the penetration probabilities of those structures associated with ruled-out hypotheses.

A web-based version of the system is under development for remote use. The current web prototype is a

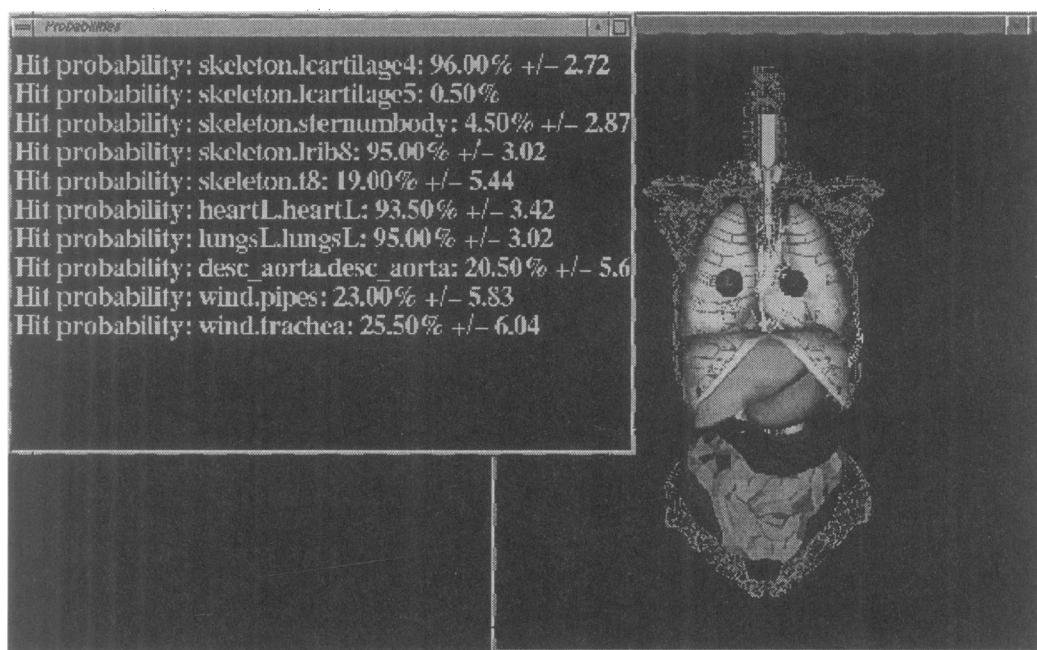


Figure 4: Penetration path hypothesis with injury probabilities

simplified 2D version of the system. We are extending this to a 3D system by modeling the anatomical structures and wound path space representations with the Virtual Reality Modeling Language (VRML). We will use written feedback from users of this extended system to gather evidence for the system's usefulness as a stand-alone tool for aiding diagnosis/education.

Reference

- [1] Anson, B. J. Atlas of Human Anatomy. W. B. Saunders, Philadelphia, 1950.
- [2] Celens, E., M. Pirlot and A. Chabotier. Terminal Effects of Bullets Based on Firing Results in Gelatin Medium and on Numerical Modeling, *The Journal of Trauma: Injury, Infection, and Critical Care*, 1996. 40(3): pp. S27 - S30.
- [3] V. DiMaio. Gunshot Wounds - Practical Aspects of Firearms, Ballistics, and Forensic Techniques. Elsevier, New York, 1985.
- [4] Eisler, R. D., A. K. Chatterjee, G. H. Burghart, and J. A. O'Keefe IV. *Casualty Assessment of Penetrating Wounds from Ballistic Trauma*. Tech Report MRC-COM-R-93-0402(R1), Mission Research Corporation: 1993.
- [5] Eisler, R. D., A. K. Chatterjee, and G. H. Burghart. Simulation and Modeling of Penetrating Wounds from Small Arms, *Health Care in the Information Age*, IOS Press and Ohmsha, 1996.
- [6] Fackler, M.L., R.F. Bellamy, and J. A. Malinowski. The Wound Profile: Illustration of Missile-Tissue Interaction. *Journal of Trauma*, 1988. 28 (Supplement 1): pp. S21-29.
- [7] Grant, J. C. Grant's Atlas of anatomy / edited by James E. Anderson, 8th ed. Williams and Wilkins, Baltimore, 1983.
- [8] Gray, H.. Gray's anatomy / edited by Peter L. Williams, 37th ed. C. Livingstone, Edinburgh, 1989.
- [9] Larsen, R. J. and M. L. Marx. An Introduction to Mathematical Statistics and Its Applications. Prentice-Hall, Englewood-Cliffs, New Jersey, 1986.
- [10] Milton, J. S., and J. C. Arnold. Introduction to Probability and Statistics: Principles and Applications for Engineering and the Computing Sciences. McGraw-Hill, New York, 1990.
- [11] Ogunyemi, O., J. Kaye, B. Webber, and J. R. Clarke. Generating Penetration Path Hypotheses for Decision Support in Multiple Trauma, *Symposium on Computer Applications in Medical Care*, 1995. 19: pp. 42 - 46.
- [12] Ogunyemi, O. Assessing the Involvement of Anatomical Structures in Penetrating Trauma Probabilistically. Technical Report, University of Pennsylvania, 1997.
- [13] Swan, K. and R. Swan. Gunshot Wounds: Pathophysiology and Management. Year Book Medical Publishers, Chicago, 1989.
- [14] Wind, G., R.W. Finley, and N. M. Rich. Three-dimensional Computer Graphic Modeling of Ballistic Injuries, *Journal of Trauma*, 1988. 28 (Supplement 1): pp. S16-20.
- [15] Yoganandan, N., F. Pintar, S. Kumaresan, D. Maiman, and S. Hargarten. Dynamic Analysis of Penetrating Trauma, *The Journal of Trauma: Injury, Infection, and Critical Care*, 1997. 42(2).